IOP Conference Series: Materials Science and Engineering

PAPER • **OPEN ACCESS**

Effects of interphase boundary anisotropy on the three-phase growth dynamics in the β(In) – In_2Bi – γ(Sn) ternary-eutectic system

To cite this article: S Mohagheghi *et al* 2019 *IOP Conf. Ser.: Mater. Sci. Eng.* **529** 012010

View the article online for updates and enhancements.

This content was downloaded from IP address 88.255.99.32 on 08/10/2019 at 15:10

IOP Conf. Series: Materials Science and Engineering **529** (2019) 012010 doi:10.1088/1757-899X/529/1/012010

Effects of interphase boundary anisotropy on the three-phase growth dynamics in the β(In) – In_2Bi – γ(Sn) ternary-eutectic system

S Mohagheghi[1], U Hecht[2], S Bottin-Rousseau[3], S Akamatsu[3], G Faivre[3], M Şerefoğlu[1]
[1] Koç University, Department of Mechanical Engineering, Rumeli Feneri Yolu, 34450, Sariyer, Istanbul, Turkey
[2] ACCESS e. V., Intzestrasse 5, D-52072 Aachen, Germany
[3] Sorbonne Université, CNRS UMR 7588, Institut des NanoSciences de Paris, Case Courrier 840, 4 Place Jussieu, 75252 Paris Cedex 05, France

mserefoglu@ku.edu.tr

Abstract. We present an experimental investigation on the effects of the interphase energy anisotropy on the formation of three-phase growth microstructures during directional solidification (DS) of the β(In)–In_2Bi–γ(Sn) ternary-eutectic system. Standard DS and rotating directional solidification (RDS) experiments were performed using thin alloy samples with real-time observation. We identified two main types of eutectic grains (EGs): (i) quasi-isotropic EGs within which the solidification dynamics do not exhibit any substantial anisotropy effect, and (ii) anisotropic EGs, within which RDS microstructures exhibit an alternation of locked and unlocked microstructures. EBSD analyses revealed (i) a strong tendency to an alignment of the In_2Bi and γ(Sn) crystals (both hexagonal) with respect to the thin-sample walls, and (ii) the existence of special crystal orientation relationships (ORs) between the three solid phases in both quasi-isotropic and anisotropic EGs. We initiate a discussion on the dominating locking effect of the In_2Bi–β(In) interphase boundary during quasi steady-state solidification, and the existence of strong crystal selection mechanisms during early nucleation and growth stages.

1. Introduction

In a directionally solidified eutectic material, the distinct crystal phases in the solid most often present several types of (special) orientation relationships (ORs). The free energy of the interphase boundaries can be substantially anisotropic, and that interfacial anisotropy, in particular, the number and the inclination of low-energy planes, depend on the OR. This has a great impact on the formation of both eutectic growth microstructures and eutectic grains (EGs) [1]. The interfacial-anisotropy effect is obviously absent from the reference, Jackson-Hunt theory of eutectic coupled-growth [2]. A major progress in this domain has been achieved thanks to the use of real-time observations in thin transparent systems [3], and, in particular, by performing real-time rotating directional solidification (RDS) experiments [4, 5]. During RDS, a thin alloy sample is slowly rotated with respect to the axis of the fixed unidirectional temperature gradient, in such a way that solidification occurs while the orientation of the crystals is continually varied. In a binary eutectic system, the trace of the interphase boundaries

Content from this work may be used under the terms of the Creative Commons Attribution 3.0 licence. Any further distribution of this work must maintain attribution to the author(s) and the title of the work, journal citation and DOI.
Published under licence by IOP Publishing Ltd

in the RDS microstructure was shown to be essentially homothetic to the equilibrium shape of the interphase boundary. As confirmed by numerical simulations [6], a weak interphase boundary anisotropy permits a fully "floating" dynamics of lamellar solidification front patterns, which allows uniformization processes that eventually lead to the formation of regular eutectic microstructures in the solid. In contrast, a strong anisotropy of the interphase boundaries can give rise to the so-called locked lamellar patterns. In the latter case, the lamellae follow a fixed direction, with the interphase boundaries aligning onto a plane that corresponds to a deep minimum in the Wulff-plot (*i.e.*, the interfacial energy-anisotropy function of the interphase boundary) [5]. Recently, an analysis, mostly by x-ray diffraction (XRD), of the crystal ORs in several eutectic grains in the In-In_2Bi alloy [7] has revealed, in brief, that (i) both quasi-isotropic and anisotropic eutectic grains exhibit special ORs, and (ii) lamellar locking mostly occurs onto atomically dense coincidence planes.

Inspiring observations and measurements have been recently made in three-phase systems, in particular the β(In)–In_2Bi–γ(Sn) alloy [8] under consideration here, and the well-known Al-Al_2Cu-Ag_2Al [9] alloy. However, a systematic study of the effects of the interfacial anisotropy and the ORs on the microstructure in such systems, which potentially present three kinds of interphase boundaries, still remains to be carried out.

In this work, we first show the microstructural evolution of the two main classes of eutectic grains, namely quasi-isotropic and anisotropic EGs, in the β(In)–In_2Bi–γ(Sn) system. In thin samples of that alloy, it is known that three-phase periodic solidification patterns exhibit an ABAC arrangement, where A = In_2Bi, B = β(In), and C = γ(Sn). In Figure 1, we show the evolution of the growth pattern of an anisotropic eutectic grain during an RDS experiment. It can be seen that the microstructure within the eutectic grain of interest is subject to substantial changes during the rotation. It successively exhibits unlocked parts with a floating behavior, and locked parts, separated by more disordered patterns. During the rotation, the position of the eutectic grain with respect to the rotation center remains globally constant. Therefore, the temperature gradient and the average growth velocity, V_{ave}, do not vary as well, and the morphological instabilities and changes of the growth pattern can be attributed to the sole variation of the orientation of the crystals with respect to the growth direction. In other words, on the light of the previous work of Refs. [4, 5], the RDS microstructure provides direct information on the Wulff-plot of the interphase boundary. More precisely, this kind of observation is similar, on a first sight, to previous observations in binary eutectic systems, but the situation for a three-phase system is more complex. It is first essential to determine the ORs between the three phases. For this purpose, we performed electron backscatter diffraction (EBSD) measurements in both quasi-isotropic and anisotropic grains. This led us to propose special ORs between the crystal phases, not only In_2Bi–β(In) and In_2Bi–γ(Sn) individually, but also with a coincidence plane common to all the three phases. Our measurements allowed us to determine that, in spite of the existence of clear ORs, the anisotropy of the In_2Bi–γ(Sn) interphase boundary is relatively weak, at least compared to that of the In_2Bi–β(In) interphase boundary which dominates the dynamics in anisotropic EGs.

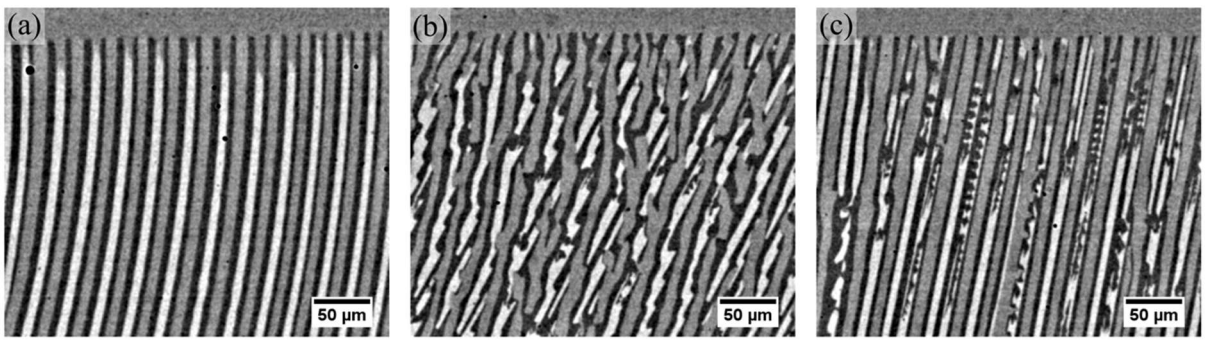


Figure 1. Evolution sequence of an anisotropic EG during an RDS experiment. (a) Unlocked, V_{ave} = 0.35 μm/s, (b) Transient, V_{ave} = 0.37 μm/s, and (c) Locked states, V_{ave} = 0.38 μm/s. G = 5.1 K/mm. RDS speed = 0.013°/s. Growth direction is counterclockwise.

2. Experimental procedure

A ternary eutectic alloy at nominal nonvariant composition, In–20.7Bi–19.1Sn (at.%) [10], was prepared from ultra-pure (99.999%) elements under Argon atmosphere. The thin-sample container, which was made out of two glass plates separated by a 13 μm-thick spacer, was filled with the molten alloy. The three phases in the eutectic solid are the body-centered tetragonal (space group number: 139) β(In), the hexagonal (space group number: 194) In_2Bi, and the hexagonal (space group number: 191) γ(Sn). Note that the indium-rich phase that is noted β here is the same phase as the one previously noted ε in Ref. [7], although the lattice parameters are different. Under optical microscope, these phases appear white, black, and gray, respectively, after numerical contrast enhancement. For gaining accuracy, we determined ourselves the crystal structures and lattice parameters of all the phases by powder x-ray diffraction. In our RDS experiments, the sample was continuously rotated (with the center of rotation being close to the solid-liquid interface) with respect to a fixed thermal gradient of 5.1 K/mm. Details of our RDS setup and experimental protocol can be found in Ref. [8]. For this study, both quasi-isotropic and anisotropic lamellar grains were processed by RDS, over several full turns, with real-time imaging. We recall that during RDS, solidification occurs one side of the sample, while the other side undergoes a directional melting. Additionally, there is a velocity ramp from the center to the edge of the sample at the solidification front. Due to this ramp, an average solidification velocity (V_{ave}) is reported in Figure 1. After a 180° rotation, the microstructure is fully renewed.

For ex-situ EBSD measurements, the glass plates were removed, without any apparent degradation of the metallic film which could then be directly exposed to the electron beam. Several high-quality crystal-orientation maps of the three phases were acquired. The area of each map was ≈ 35×10^3 μm^2 with a pixel size equal to 0.42 μm. The sample was aligned inside the scanning electron microscope (SEM) so that the axis of the temperature gradient during solidification was nearly parallel to the so-called rolling direction (RD) of the EBSD.

3. Results and discussions

In the RDS microstructure of Figure 2, two different regions can be distinguished according to their microstructures, namely, a central region with quasi-isotropic grain, and a distal region with anisotropic grain. The coexistence of the two types of growth dynamics in the same experiment again brings clear evidence of the influence of the interphase anisotropy.

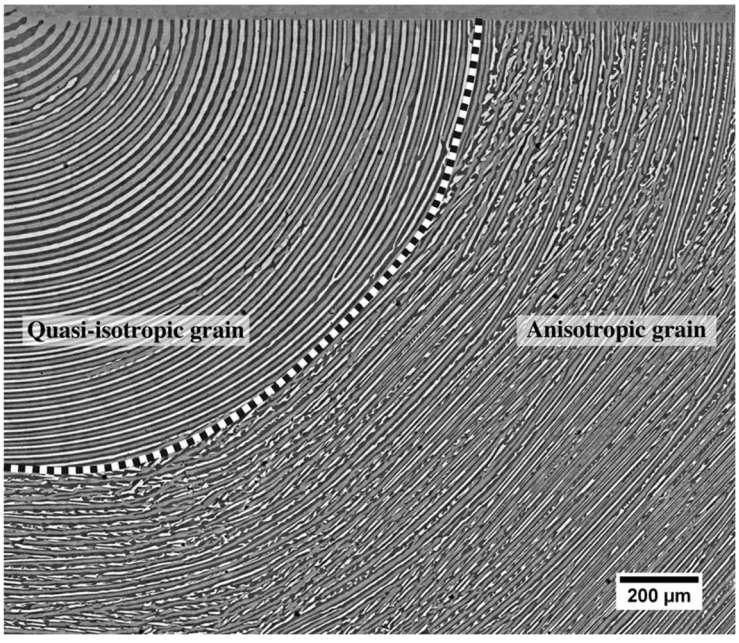


Figure 2. Quasi-isotropic and anisotropic EGs obtained in an RDS experiment. RDS speed = 0.013°/s. Growth direction is counterclockwise. Dashed line shows the grain boundary.

3.1. Identification of ORs in quasi-isotropic grains

We first focus on the floating region. In a quasi-isotropic grain, the lamellae grow essentially perpendicular to the average growth front. During RDS, the trajectories of the triple-junctions in the reference frame of the sample smoothly follow concentric circles, or nearly circular curves, within the possible effect of a small anisotropy and local deviations caused by spacing adjustment mechanisms due to the complex dynamics during RDS (Ex: spatial growth velocity ramp along the front, misalignment of the center of rotation, influence of grain boundary). In another sample, after a full rotation, the floating nature of the growth dynamics was further tested by standard DS without rotation (Figure 3). As expected, a regular ABAC lamellar structure formed in continuity with the RDS structure.

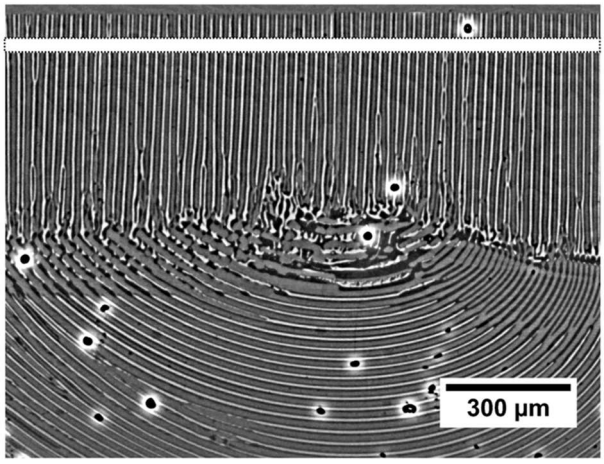


Figure 3. Evolution of the quasi-isotropic eutectic grain during RDS and DS experiments. The image on top shows the solid/liquid interface after 1500 µm growth with DS. RDS speed = 0.026°/s, DS speed = 0.5 µm/s.

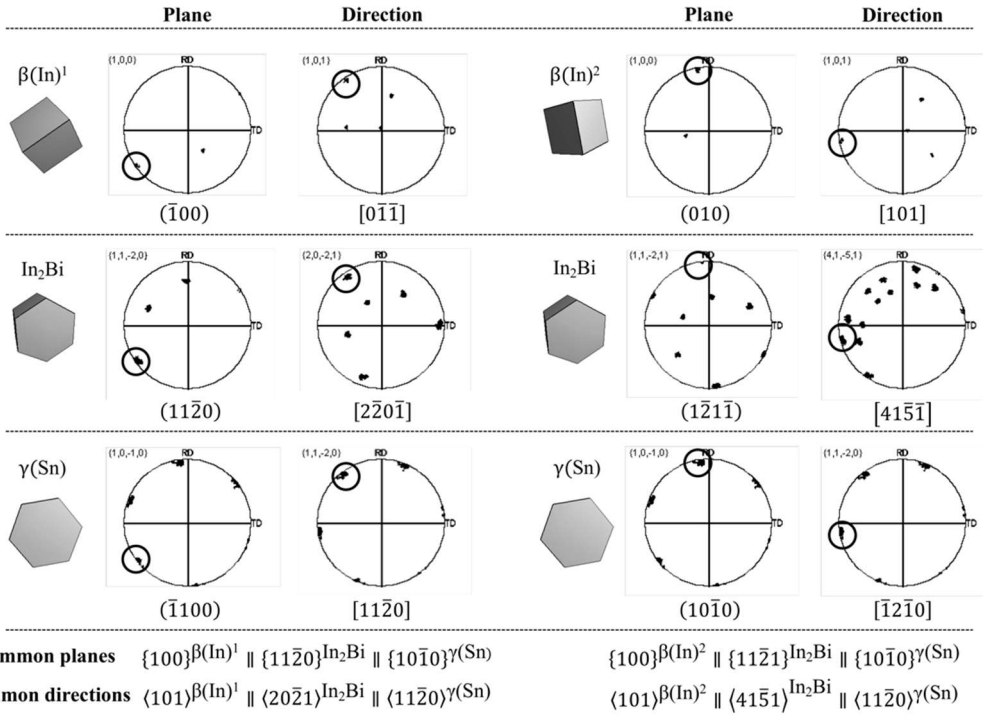


Figure 4. Crystal mimics and pole figures corresponding to the identified ORs of the quasi-isotropic pattern shown in Figure 3. EBSD maps are obtained from DS and RDS regions and both regions contain $\beta(In)^1$ and $\beta(In)^2$ phases. Common planes and directions are given below the pole figures.

We performed EBSD measurements in both the RDS and DS microstructures shown in Figure 3. We found that both In_2Bi and γ(Sn) phases keep one and the same orientation over the entire explored areas. In contrast, the β(In) phase presents two different orientations, named as $\beta(In)^1$ and $\beta(In)^2$, in both RDS and DS regions. In other words, the floating region is composed of two distinct types of eutectic grains, the difference between them being solely the orientation of the β(In) phase. The corresponding pole figures are shown in Figure 4 along with the crystal mimics of the three phases. In both $\beta(In)^1$–In_2Bi–γ(Sn) and $\beta(In)^2$–In_2Bi–γ(Sn) grains, the basal (0001) plane of the γ(Sn) crystals is parallel to the sample plane. The basal plane of the In_2Bi crystals is slightly inclined from the sample plane. From the pole figures extracted from the EBSD measurements, two special ORs between In_2Bi and γ(Sn) can be plausibly proposed, namely, $\{11\bar{2}0\}$ In_2Bi ∥ $\{10\bar{1}0\}$ γ(Sn), and $\{11\bar{2}1\}$ In_2Bi ∥ $\{10\bar{1}0\}$ γ(Sn), respectively, with angular departures between the involved In_2Bi and γ(Sn) lattice planes being less than about 2°. It is noticeable that those planes are perpendicular to the sample plane. We also identified ORs between In_2Bi and both $\beta(In)^1$ and $\beta(In)^2$. Both of them involve the $\{100\}$ family planes of the β(In) crystals, namely: $(11\bar{2}0)$ In_2Bi ∥ $(\bar{1}00)$ $\beta(In)^1$, and $(1\bar{2}1\bar{1})$ In_2Bi ∥ (010) $\beta(In)^2$, respectively. Again, those planes are perpendicular to the sample plane.

A first conclusion from the above observations is that there is no clearly remarkable manifestation of the ORs in the quasi-isotropic EGs. In other words, in the quasi-isotropic grains, there is no measurable tendency of any preferred alignment of the interphase boundaries with the coincidence planes involved in the identified ORs, which indicates that these coincidence planes are associated to very shallow minima in the Wulff-plot. This phenomenon has also been previously found in the binary In-In_2Bi system [7]. In addition, our analysis shows that all the three phases have a common plane in coincidence as emphasized in Figure 4, which was not expected a priori. The generalization of this result has to be confirmed by more systematic observations in different samples. It would evidence the existence of particular, and strong crystal orientation selection mechanisms at play during the early nucleation and growth stages of eutectic solidification (including the alignment of the hexagonal crystals with respect to the sample walls).

3.2. Identification of ORs in an anisotropic grain

We now focus on the locked region of the RDS microstructure shown in Figure 2. We acquired EBSD maps in different regions with distinct microstructural features, namely unlocked, transient, and locked (Note that the EBSD measurements have been made after several RDS turns; at this final stage, the microstructure shown in Figure 2 had been melted, and replaced by new but similar ones). The results of the EBSD measurements and the proposed ORs are shown in Figure 5. We observed that the crystal orientations do not vary, within the experimental accuracy, by following continuously group of lamellae. In other words, even though the microstructures are highly dissimilar in unlocked, transient, and locked states, the same OR is preserved, as expected. Interestingly, in this eutectic grain, not only the γ(Sn) crystals (as in the quasi-isotropic EGs analyzed above) but also the In_2Bi crystals are oriented in such a way that their basal (0001) plane lies parallel to the sample plane. In addition, the prismatic planes of both γ(Sn) and In_2Bi crystals (which are therefore perpendicular to the sample plane) are strictly parallel with each other. In brief, the hexagonal crystals of the two phases have the same orientation. This defines a remarkable and unusual, high-symmetry OR between the two hexagonal phases even though the lattice parameters are substantially different. We also identified that $\{112\}$ family planes of β(In) and the $\{10\bar{1}0\}$ family planes of In_2Bi, thus of γ(Sn) as well, are parallel with each other.

In the RDS microstructure of the anisotropic grain, we observed some facets along the In_2Bi-β(In) interphase boundaries. Some facets are well aligned with the identified coincidence planes. No clear facets are observed along the In_2Bi-γ(Sn) interphase boundaries. As it was suggested from the previous study [8], the anisotropy of the In_2Bi-β(In) interface is responsible for the overall locking dynamics of the eutectic grain.

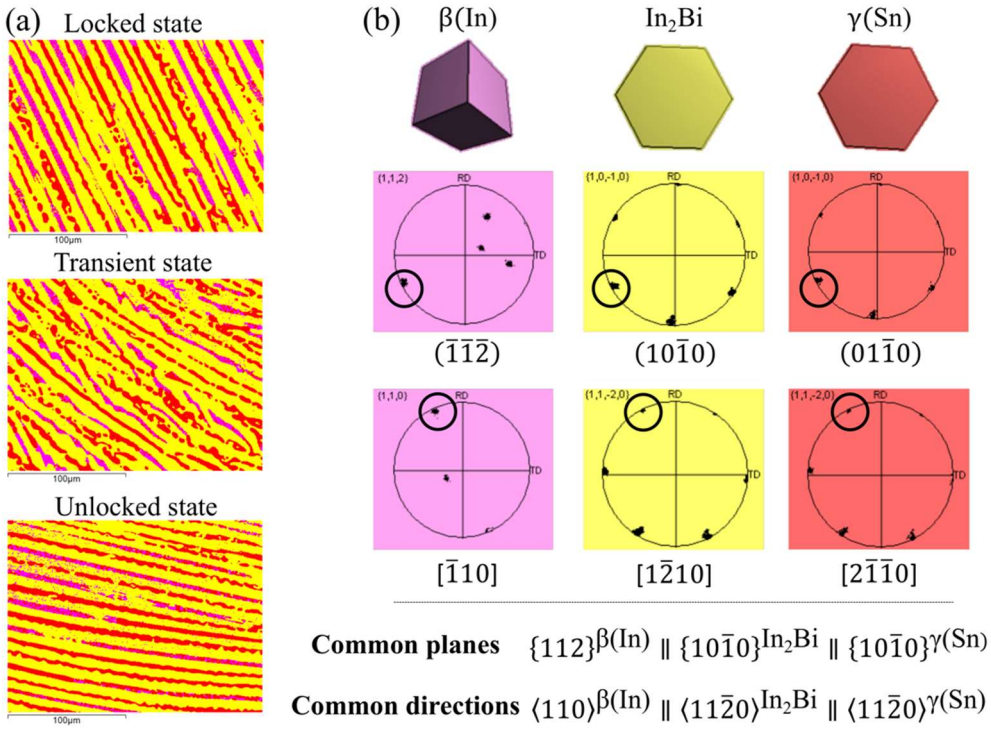


Figure 5. Crystal mimics and pole figures corresponding to the identified OR of unlocked, transient, locked states of the anisotropic grain. Common planes and directions are summarized as well.

Summary and conclusions

We used the RDS method for in-situ observation of the microstructure growth dynamics in thin samples of β(In)-In_2Bi-γ(Sn) three-phase system, and ex-situ EBSD analysis for determining the orientation of the crystals growing in a coupled manner. We have selected samples in which quasi-isotropic and anisotropic grains were clearly distinguishable, on a microstructural basis. We could identify special ORs all of which involve dense common planes in both cases between the three phases. In the quasi-isotropic grains, special ORs could be identified, but the interfacial anisotropies of both In_2Bi-β(In) and In_2Bi-γ(Sn) interphase boundaries remain weak. Due to this weakness, the floating growth dynamics are insensitive to the ORs. In the anisotropic grain, careful EBSD maps taken from three different states, namely, unlocked, transient, and locked, reveal that the crystal orientations stay constant during the evolution of the grain in the RDS experiment. More specifically, despite significant microstructural dissimilarities in these states, ORs are identical. In this grain, since the interphase boundaries of the In_2Bi-β(In) in the locked state are well-aligned with the identified common plane, this interphase is suggested to dominate the dynamics, and a locking effect is observed to occur in the vicinity of the coincidence family planes, namely, {112}β(In) ∥ {10$\bar{1}$0}In_2Bi. During solidification, the trajectory of the In_2Bi-γ(Sn) interphase boundaries is more or less slaved to the evolution dynamics imposed by the anisotropy of the In_2Bi-β(In) interphase boundaries. We can assume that the interfaces remain perpendicular to the sample walls as it is usually the case in a thin-sample geometry and in steady-state conditions. The anisotropy thus merely corresponds to a section of the Wulff-plot of the considered interface with the sample plane. For the In_2Bi and γ(Sn) crystals, which have basal planes nearly aligned with the sample plane, a weak anisotropy is thus apparently associated with the hexagonal symmetry of those lattice planes. The alignment of the hexagonal In_2Bi and γ(Sn) crystals in such a way that the basal planes are parallel to the sample plane is a remarkable feature. The selection mechanism at play is still unclear. It must obviously be determined during the early stages of the three-phase solid formation, including heterogeneous nucleation and competitive growth after the sample filling process. Further

EBSD and XRD analyses are needed to a more comprehensive identification of the locking planes and the associated ORs in this system.

Acknowledgments
This work was supported by European Commission Marie Curie Career Integration Grant FP7-PEOPLE-2012-CIG (NEUSOL 334216) and TÜBİTAK 3501 (Grant no: 212M013). The authors would like to thank Nicolas Casaretto for helping us for XRD measurements. Some of us would like to acknowledge funding through the M-Era.Net Project ANPHASES (UH: DFG HE 6938/2-1; SBR and SA: ANR-14-MERA-0004).

References
[1] Hogan L M, Kraft R W and Lemkey F D 1971 *Adv. Mater. Res.* **5** 83-126
[2] Jackson K A and Hunt J D 1966 *Trans. Metall. Soc. AIME* **236** 1129-42
[3] Caroli B, Caroli C, Faivre G and Mergy J 1992 *J. Cryst. Growth* **118** 135-50
[4] Akamatsu S, Bottin-Rousseau S, Serefoglu M and Faivre G 2012 *Acta Mater.* **60** 3199-205
[5] Akamatsu S, Bottin-Rousseau S, Şerefoğlu M and Faivre G 2012 *Acta Mater.* **60** 3206-14
[6] Ghosh S, Choudhury A, Plapp M, Bottin-Rousseau S, Faivre G and Akamatsu S 2015 *Phys. Rev. E* **91** 022407
[7] Bottin-Rousseau S, Senninger O, Faivre G and Akamatsu S 2018 *Acta Mater.* **150** 16-24
[8] Mohagheghi S and Şerefoğlu M 2018 *Acta Mater.* **151** 1-11
[9] Steinmetz P, Dennstedt A, Şerefoğlu M, Sargin I, Genau A and Hecht U 2018 *Acta Mater.* **157** 96-105
[10] Witusiewicz V T, Hecht U, Bottger B and Rex S 2007 *J. Alloys Compd.* **428** 115-24